Reversal of muscle insulin resistance by weight reduction in young, lean, insulin-resistant offspring of parents with type 2 diabetes

Kitt Falk Petersen[a], Sylvie Dufour[a,b], Katsutaro Morino[a,b], Peter S. Yoo[c], Gary W. Cline[a], and Gerald I. Shulman[a,b,d,1]

[a]Department of Internal Medicine, [c]Department of Surgery, [d]Department of Cellular and Molecular Physiology, and [b]the Howard Hughes Medical Institute, Yale University School of Medicine, New Haven, CT 06536

Contributed by Gerald I. Shulman, April 5, 2012 (sent for review February 6, 2012)

To examine the role of intramyocellular lipid (IMCL) accumulation as well as circulating cytokines, branched-chain amino acids and acylcarnitines in the pathogenesis of muscle insulin resistance in healthy, young, lean insulin-resistant offspring of parents with type 2 diabetes (IR offspring), we measured these factors in plasma and used ^{1}H magnetic resonance spectroscopy to assess IMCL content and hyperinsulinemic-euglycemic clamps using [6,6-$^2H_2$] glucose to assess rates of insulin-stimulated peripheral glucose metabolism before and after weight reduction. Seven lean (body mass index < 25 kg/m^2), young, sedentary IR offspring were studied before and after weight stabilization following a hypocaloric (1,200 Kcal) diet for ∼9 wks. This diet resulted in an average weight loss of 4.1 ± 0.6 kg (P < 0.0005), which was associated with an ∼30% reduction of IMCL from 1.1 ± 0.2% to 0.8 ± 0.1% (P = 0.045) and an ∼30% improvement in insulin-stimulated muscle glucose uptake [3.7 ± 0.3 vs. 4.8 ± 0.1 mg/(kg–min), P = 0.01]. This marked improvement in insulin-stimulated peripheral insulin responsiveness occurred independently of changes in plasma concentrations of TNF-α, IL-6, total adiponectin, C-reactive protein, acylcarnitines, and branched-chain amino acids. In conclusion, these data support the hypothesis that IMCL accumulation plays an important role in causing muscle insulin resistance in young, lean IR offspring, and that both are reversible with modest weight loss.

adipocytokines | insulin sensitivity index | mitochondria | diacylglycerols | visceral fat

Insulin resistance is the best predictor for an increased risk of developing type 2 diabetes (T2D) yet the cellular mechanism responsible for the insulin resistance remains unknown (1–4). Previous studies have demonstrated that skeletal muscle insulin resistance, due to defects in insulin-stimulated glucose transport activity resulting in decreased muscle glycogen synthesis, is the earliest defect detectable in healthy, young, lean insulin-resistant offspring of parents with T2D (IR offspring) (5–8). Furthermore, previous studies have found a strong relationship between intramyocellular lipid (IMCL) content assessed by ^{1}H magnetic resonance spectroscopy (MRS) and muscle insulin resistance (9–13), suggesting that intracellular lipid metabolites (e.g., diacylglycerols, ceramides) might be a causal factor in its pathogenesis (14–16).

To directly examine this hypothesis, we studied whether modest weight reduction would result in a reduction in IMCL content in lean IR offspring, and if so whether this reduction in IMCL would be associated with improvements in insulin-stimulated skeletal muscle glucose uptake, assessed by a hyperinsulinemic-euglycemic clamp. Furthermore, because changes in inflammatory adipocytokines (17–20), branched-chain amino acids (21, 22), and acylcarnitines (23) have also been implicated in the pathogenesis of insulin resistance, we also measured plasma levels of these factors before and after this modest weight-loss intervention.

Results

The IR offspring were markedly insulin-resistant, as reflected by their insulin sensitivity index (ISI) being in the lower ISI quartile (<3.68 × 10^{-4} dL/min per μU/mL) for similar young lean, healthy, sedentary individuals (24). During the caloric restriction period the subjects lost on average 4.1 ± 0.6 kg, or ∼6% of their initial body weight, and body mass index (BMI) decreased from 24.2 ± 0.6 to 22.8 ± 0.5 kg/m^2 (Table 1), which was independent of any changes in physical activity as assessed by pedometer (1.4 ± 0.3 *K*m/d before weight loss vs. 1.5 ± 0.2 *K*m/d after weight loss; P = 0.87). This modest reduction in body weight was associated with an 11% reduction in whole body-fat mass and a marked 30% reduction in IMCL content (Fig. 1*A*). In contrast, there were no significant reductions in intra-abdominal fat volume, liver fat content, or lean body mass following this weight reduction (Table 1). Interestingly, lipid droplet density in skeletal muscle, assessed by electron microscopy, increased by ∼60% despite the decrease in IMCL content (Table 1). There were no changes in muscle mitochondrial density following weight reduction (Table 1).

After weight reduction the ISI increased by ∼60%, demonstrating reversal of their whole-body insulin resistance (Table 2). To assess which organ was mostly responsible for the reversal of their whole-body insulin resistance, we performed hyperinsulinemic-euglycemic clamp studies in combination with infusions of [6,6-$^2H_2$]glucose and [$^2H_5$]glycerol to assess insulin action in liver, skeletal muscle, and fat cells. Consistent with the ∼60% increase in the ISI index following the weight reduction, we observed an approximately ∼30% increase in the rate of insulin-stimulated glucose uptake during the hyperinsulinemic-euglycemic clamp (Table 3). This increase in insulin-stimulated glucose metabolism could entirely be attributed to increased insulin-stimulated peripheral glucose uptake (Fig. 1*B*) as a result of increased nonoxidative glucose metabolism because hepatic glucose production was completely suppressed during the hyperinsulinemic-euglycemic clamp both before and after weight reduction (Table 3).

Consistent with the reduction in body fat mass, fasting plasma concentrations of leptin decreased by 19 ± 6% after the weight loss in the IR offspring (Table 2). In addition, plasma alanine concentrations decreased by 57% following weight loss. In contrast, there were no detectable changes in plasma levels of TNF-α, IL-6, total adiponectin, acylcarnitines, uric acid, branched-chain amino acids (Table 2), or basal and insulin-suppressed rates of glycerol turnover during the clamp (Table 3) following weight loss.

Discussion

Skeletal muscle insulin resistance is the earliest metabolic defect observed in young, lean IR offspring, yet the mechanism responsible for the insulin resistance is unknown. In this regard muscle insulin resistance in these individuals is strongly associated

Author contributions: K.F.P. and G.I.S. designed research; K.F.P., S.D., K.M., P.S.Y., and G.W.C. performed research; K.F.P., S.D., K.M., G.W.C., and G.I.S. analyzed data; and K.F.P., S.D., K.M., G.W.C., and G.I.S. wrote the paper.

The authors declare no conflict of interest.

Freely available online through the PNAS open access option.

[1]To whom correspondence should be addressed. E-mail: gerald.shulman@yale.edu.

Table 1. Body weight, BMI, and body composition before and after weight loss

Variable	Before weight loss	After weight loss	*P* value
Body weight (kg)	67.5 ± 3.8	63.4 ± 3.6	<0.0005
BMI (kg/m^2)	24.2 ± 0.6	22.8 ± 0.5	<0.0005
Fat mass (kg)	19.4 ± 1.2	17.3 ± 1.3	<0.05
Lean body mass (kg)	48.1 ± 3.9	46.1 ± 3.9	<0.005
Intra-abdominal fat volume (mL)*	337 ± 68	251 ± 34	0.20
Subcutaneous fat volume (mL)*	1,519 ± 95	1,316 ± 147	0.10
Liver fat content (%)*	0.34 ± 0.02	0.27 ± 0.04	0.12
IMCL droplet density (%)	24.0 ± 16.7	39.0 ± 18.3	<0.04
Muscle mitochondrial density (%)	1.87 ± 0.36	1.61 ± 0.46	0.24

Data are expressed as mean ± SEM.
*n = 5.

with increased IMCL content (9, 11, 13, 15). To directly examine the potential role of IMCL, as a marker for other intracellular lipid intermediates (e.g., diacylglycerols, ceramides) in the pathogenesis of muscle-specific insulin resistance in IR offspring, we examined whether we could reduce IMCL with a modest weight-loss intervention, and if so, whether this reduction in IMCL would be associated with an improvement in insulin-stimulated peripheral glucose uptake. In addition, because recent studies have also implicated a potential role for increased concentrations of acylcarnitines (23, 25), branched-chain amino acids (21, 22), and adipocytokines (17, 19, 20, 26) in this process, we also measured these metabolites and cytokines before and after weight loss. Using this approach, we found that a modest weight loss of ∼5 kg resulted in an ∼30% reduction in IMCL content, which was associated with an ∼30% increase in insulin-stimulated peripheral glucose uptake.

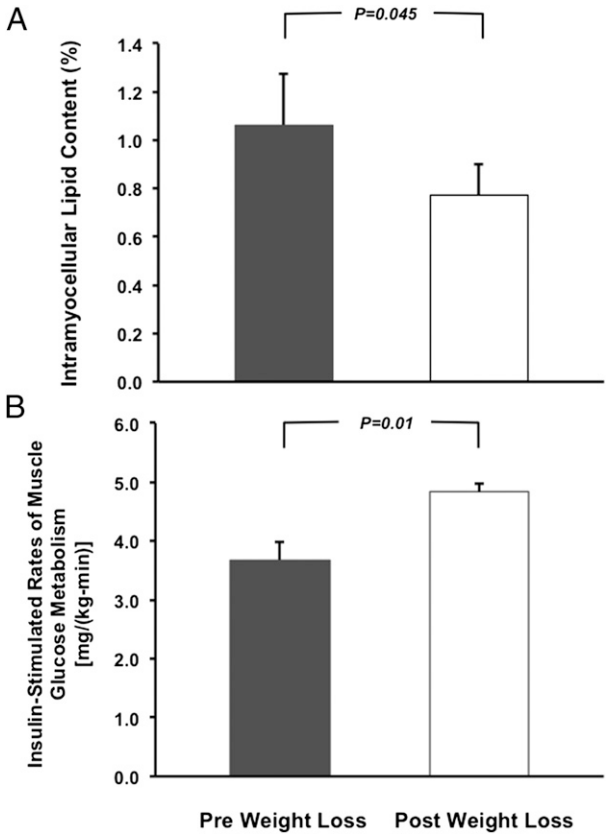

Fig. 1. Changes in IMCL content (*A*) and rates of insulin-stimulated peripheral glucose metabolism (*B*) before and after weight reduction.

These young, lean IR offspring had very low hepatic lipid content (∼0.3%) and complete suppression of hepatic glucose production, both before and after the weight reduction.

In contrast to the observed reductions in IMCL in the IR offspring, we did not observe any reductions in circulating plasma levels of TNF-α, IL-6, total adiponectin, C-reactive protein, branched-chain amino acids, or acylcarnitines in the IR offspring following weight reduction, suggesting that these factors do not play a major role in either causing or alleviating their insulin resistance following weight reduction.

Taken together, these findings support the hypothesis that accumulation of IMCL plays a causal role in the pathogenesis of skeletal muscle insulin resistance in young, lean IR offspring (14, 16). These findings are consistent with previous studies in which reductions in ectopic lipid content in muscle and liver were associated with reversal of insulin resistance in theses organs in patients with generalized lipodystrophy following leptin treatment, and specific reductions in hepatic lipid content and reversal of hepatic insulin sensitivity in obese T2D patients following modest weight reduction (27–29).

The cellular mechanism by which IMCL accumulation causes muscle insulin resistance in humans is not well established. Although IMCL as assessed by ^{1}H NMR, which mostly reflects triglyceride, is strongly associated with muscle insulin resistance (9–13), studies in rodents have disassociated increases in total intramuscular triglyceride content from muscle insulin resistance (30). Instead, studies in rodents have implicated ceramides (31) and diacylglycerols (32–34) as the trigger for lipid-induced insulin resistance in skeletal muscle. Increased muscle diacylglycerol content has been shown to activate PKCθ, resulting in increased insulin receptor substrate serine-1101 phosphorylation, decreased insulin-stimulated IRS-1 tyrosine phosphorylation, and reduced insulin-stimulated glucose uptake in skeletal muscle (32–35). Whether the same mechanism is responsible for lipid-induced insulin resistance in human muscle is less clear, in that Itani et al. (12) found that muscle insulin resistance induced by a lipid infusion resulted in an increase in intramuscular diacylglycerol content and increased membrane associated PKCβ-II and -δ; however, these results were not replicated in a recent study by Høeg et al. (36).

Increases in IMCL content in the IR offspring can be attributed to an imbalance in rates of fatty acid delivery/uptake by the myocyte relative to the rates of mitochondrial fatty acid oxidation, where rates of fatty acid delivery/uptake by the myocyte exceed the rates of mitochondrial fatty acid oxidation, resulting in an increase in intramyocellular content of long chain fatty acyl CoAs, which are the precursors for the synthesis of diacylglycerols and triacylglycerols (30). In this regard, previous studies have found that IR offspring have an ∼30% reduction in basal rates of mitochondrial ATP production (11) and TCA cycle oxidation (11, 37) in muscle, which could be attributed to a 38% reduction in mitochondrial content assessed by electron

Table 2. Fasting plasma metabolite and adipocytokine concentrations in IR offspring before and after weight loss

Variable	Before weight loss	After weight loss	*P* value
Glucose (mmol/L)	5.0 ± 0.2	4.7 ± 0.2	0.02
Insulin (pmol/L)	104.8 ± 9.4	73.4 ± 7.8	0.07
C-peptide (nmol/L)	0.47 ± 0.05	0.35 ± 0.06	0.17
Lactate (mmol/L)	1.05 ± 0.13	0.73 ± 0.07	0.09
Total cholesterol (mmol/L)	4.5 ± 0.2	4.2 ± 0.1	0.18
HDL cholesterol (mmol/L)	1.6 ± 0.1	1.7 ± 0.1	0.21
LDL cholesterol (mmol/L)	2.5 ± 0.2	2.1 ± 0.2	0.13
Triglycerides (mmol/L)	0.9 ± 0.2	0.9 ± 0.2	0.37
Fatty acids (mmol/L)	0.50 ± 0.06	0.42 ± 0.10	0.30
Uric acid (μmol/L)	189.0 ± 22.5	213.0 ± 23.0	0.14
Leptin (ng/ml)	13.4 ± 2.9	10.8 ± 2.4	0.04
IL-6 (pg/mL)	1.40 ± 0.51	1.00 ± 0.25	0.46
Total adiponectin (μg/mL)	12.3 ± 2.5	12.3 ± 2.7	0.86
TNF-α (pg/mL)	1.44 ± 0.14	1.43 ± 0.28	0.99
C-reactive protein (mg/L)	0.49 ± 0.22	0.45 ± 0.24	0.23
ISI (10^{-4} dL/min per μU/mL)	2.54 ± 0.15	4.08 ± 0.67*	0.05
Acylcarnitines (μmol/L)	14.4 ± 4.0	17.3 ± 3.6	0.44
Total protein (g/dL)	5.75 ± 0.17	5.68 ± 0.17	0.69
Glycine (mmol/L)	0.20 ± 0.02	0.21 ± 0.03	0.77
Leucine (mmol/L)	0.10 ± 0.01	0.09 ± 0.01	0.34
Isoleucine (mmol/L)	0.05 ± 0.01	0.05 ± 0.01	0.98
Valine (mmol/L)	0.16 ± 0.02	0.16 ± 0.02	0.93
Tyrosine (mmol/L)	0.07 ± 0.01	0.07 ± 0.01	0.18
Phenylalanine (mmol/L)	0.04 ± 0.01	0.04 ± 0.01	0.10
Aspartate (mmol/L)	0.02 ± 0.01	0.02 ± 0.01	0.20
Glutamine/glutamate (mmol/L)	0.23 ± 0.03	0.21 ± 0.02	0.45
Alanine (mmol/L)	0.33 ± 0.03	0.21 ± 0.01	0.009

*n = 6.

microscopy (8). Two microarray studies suggested that reductions in peroxisome proliferator-activated γ-coactivator 1α might be responsible for reduced mitochondrial function in the muscle of T2D patients (38, 39) and their first-degree relatives (39); however, these results have not been replicated in lean IR offspring (8). More recently, using a similar microarray approach, Morino et al. found decreased expression of lipoprotein lipase associated with increased IMCL content and reduced mitochondrial content in the muscle of healthy, lean, IR offspring (40). Furthermore, they found that lipoprotein lipase knockdown in muscle cells decreased mitochondrial content by effectively decreasing eicosapentaenoic acid delivery and uptake by the myocyte and subsequent activation of peroxisome proliferator-activated receptor-δ, a known regulator of mitochondrial biogenesis (41). In the present study, we found a similar reduction in mitochondrial density in the IR offspring as previously described (8, 41). Furthermore, we found that modest weight reduction resulted in a decrease in IMCL associated with an increase in insulin-stimulated peripheral glucose metabolism, which were independent of changes in mitochondrial density. Taken together, these data demonstrate that reductions in IMCL can occur independently of changes in mitochondrial content, most likely because of decreases

Table 3. Basal and insulin-stimulated rates of glucose and glycerol turnover, glucose and lipid oxidation, and respiratory quotient before and after weight loss

	Before weight loss	After weight loss	*P* value
Basal state			
Glucose production [mg/(kg-min)]	2.07 ± 0.08	1.93 ± 0.16	0.54
Glucose oxidation [mg/(kg-min)]	1.49 ± 0.15	1.15 ± 0.28	0.11
Lipid oxidation [mg/(kg-min)]	1.07 ± 0.08	1.20 ± 0.16	0.20
Respiratory quotient	0.80 ± 0.01	0.79 ± 0.02	0.04
Glycerol turnover (μmol/min)	0.23 ± 0.05	0.23 ± 0.03	0.99
Hyperinsulinemic-euglycemic clamp			
Glucose infusion rate [mg/(kg-min)]	3.26 ± 0.33	4.49 ± 0.22	0.02
Glucose production [mg/(kg-min)]	0.21 ± 0.07	0.02 ± 0.10	0.06
Muscle glucose disposal [mg/(kg-min)]	3.68 ± 0.31	4.84 ± 0.14	0.01
Glucose oxidation [mg/(kg-min)]	2.60 ± 0.35	1.55 ± 0.42	0.11
Lipid oxidation [mg/(kg-min)]	0.59 ± 0.09	0.64 ± 0.19	0.45
Nonoxidative glucose metabolism [mg/(kg-min)]	1.39 ± 0.45	3.29 ± 0.40	<0.02
Respiratory quotient	0.87 ± 0.02	0.88 ± 0.03	0.66
Glycerol turnover (μmol/min)	0.09 ± 0.01	0.10 ± 0.01	0.72
Insulin suppression of glycerol turnover (%)	98 ± 1	98 ± 1	0.29

in substrate delivery and uptake by the myocyte during the weight-loss regimen. These results, however, still do not answer the question as to whether reductions in mitochondrial content in the IR offspring are a primary or secondary event. Nevertheless reduced mitochondrial content in muscle of the IR offspring would be expected to promote net IMCL metabolite accumulation and exacerbate lipid-induced muscle insulin resistance, regardless of whether it is a primary or secondary phenomenon.

In summary, these data support the hypothesis that IMCL accumulation plays an important role in causing muscle insulin resistance in young, lean IR offspring, and that both are reversible with modest weight loss. Furthermore, in contrast to reductions in IMCL observed with weight loss, reversal of muscle insulin resistance in the IR offspring occurred independently of any changes in branched-chain amino acids, acylcarnitines, and circulating adipocytokines, suggesting that these factors do not play a major role in causing muscle insulin resistance in these individuals.

Methods

Subjects. We recruited seven (six women: two Black and four Caucasian; one man: Asian), 25 ± 4-y-old, healthy, lean, nonsmoking insulin-resistant individuals with at least one parent with T2DM (IR offspring) from an ongoing insulin-sensitivity screening study in the Greater New Haven, CT area. Insulin sensitivity in these individuals was assessed by performing an oral glucose tolerance test and calculating an ISI, as previously described (42). Insulin resistance in these individuals was defined by their being in the lowest quartile of ISI ($ISI \leq 3.68 \times 10^{-4}$ dL/min per μU/mL) in a population of subjects of similar age, BMI, and physical activity (24). All subjects had a sedentary lifestyle without any regular exercise regimen and, except for birth-control pills, were not taking any medications. Physical activity was assessed using a standard questionnaire and by monitoring activity over 3 consecutive days (Sportline). Body composition was assessed by dual-energy X-ray absorptiometry (43), bioelectrical impedance (Tanita BC-418; Tanita), and MRI, as described below. Only subjects with normal glucose tolerance, no MRS contraindications, and willing to undergo a weight-loss regimen were included in the study. The protocol was approved by the Human Investigation Committee at Yale University School of Medicine and informed, written consent was obtained from all subjects after the aims and potential risks were explained to them.

Oral Glucose Tolerance Test. At the time of study entry all subjects had normal fasting plasma glucose concentrations and normal glucose tolerance as determined by a 3-h 75-g oral glucose tolerance test, which was performed before and after the weight loss regimen and the ISI was calculated to estimate insulin sensitivity.

^{1}H MRS Assessment of Intramyocellular, Extramyocellular, and Hepatic Lipid Content. Within 3 d before the start of the weight-loss studies, at regular intervals during the weight loss, and within 3 d after completion of the weight-loss studies, intra- and extramyocellular and hepatic lipid contents were measured using ^{1}H MRS at 4T (Bruker), as previously described (24). Muscle lipid content was measured in the soleus muscle using an 8.5-cm diameter circular ^{13}C surface coil with twin, orthogonal circular 13-cm ^{1}H quadrature coils. The probe was tuned and matched and scout images of the lower leg were obtained to ensure correct positioning of the subject and to define an adequate volume for localized shimming using the FASTMAP procedure (44). The liver triglyceride content was measured by ^{1}H respiratory-gated STEAM spectroscopy in a $15 \times 15 \times 15$-mm^3 voxel. Acquisition was synchronized to the respiratory cycle and triggered at the end of expiration. A water-suppressed lipid spectrum and a lipid-suppressed water spectrum were acquired in three different locations of the liver to account for liver inhomogeneity. A minimum of six spectra were acquired for each subject and the total lipid content was averaged and calculated. In addition, hepatic lipid content was corrected for transverse relaxation, using the transverse relaxation times of 22 ms for water and 44 ms for lipid, as previously described (45).

MRI Measurements of Visceral and Subcutaneous Fat Volumes. A MR image of the trunk was acquired in each subject using a Siemens Sonata 1.5T Instrument (multibreath-hold T1-weighted acquisition; field of view: 38.0 × 38.0 cm; matrix = 256 × 256; in-plane resolution = 1.48 mm; 50 contiguous slices; 5-mm slice thickness). Following slice intensity homogeneity correction, intra-abdominal and subcutaneous fat was interactively segmented in each slice using the Yale BioImage Suite software package (http://www.bioimagesuite.org) and the segmentation map was summed for the entire trunk to generate volume measurements (24).

Hyperinsulinemic-Euglycemic Clamp. For 3 d before the before and after weight-loss studies, the subjects were instructed to eat a regular eucaloric diet (55% carbohydrate, 15% protein, 30% fat) with the calories evenly divided between breakfast, lunch, and dinner and to provide dietary records. Subjects were admitted to the Yale Center for Clinical Investigation Hospital Research Unit the evening before each study, dinner was taken at 7:00 PM, and the subjects remained fasting from 10:00 PM until the end of the study the following day. At 4:00 AM a polyethylene catheter was inserted into an antecubital vein for the study infusions. A 3-h primed (4.2 mg/m^2) continuous [2.1 mg/(m^2-min)] infusion of [6,6-^{2}H$_2$]glucose along with a constant infusion of [^{2}H$_5$]glycerol [1.2 mg/(m^2-min)] was started at 5:00 AM to assess rates of basal endogenous glucose production and whole body glycerol turnover, respectively (11). At 7:00 AM one of the subject's hands was placed in a heated box and warmed to 55 °C (to "arterialize" the venous blood) and a polyethylene catheter was inserted retrogradely into one of the hand veins for blood collections (11). During the final 30 min of the baseline period blood samples were collected for determination of [6,6-^{2}H$_2$]glucose and [^{2}H$_5$]glycerol enrichments, as well as for plasma glucose, insulin, C-peptide, nonesterified fatty acid, IL-6, TNF-α, total adiponectin, leptin, acylcarnitine, and amino acid concentrations.

A 3-h euglycemic-hyperinsulinemic clamp was initiated by a two-step primed infusion of insulin [80 mU/(m^2-min) for 5 min, 60 mU/(m^2-min) for 5 min] immediately followed by a continuous infusion of insulin at a rate of 20 mU/(m^2-min) (human recombinant insulin, Novolin U-100 Regular; Novo-Nordisk, NJ) (11). Euglycemia and plasma [6,6-^{2}H$_2$]glucose enrichments were maintained with a variable infusion of D-20 containing [6,6-^{2}H$_2$]glucose (11, 46). Blood was collected every 5–10 min for determination of plasma glucose and lactate concentrations and every 30 min for measurements of plasma insulin, fatty acids, and [6,6-^{2}H$_2$]glucose and [^{2}H$_5$]glycerol enrichments.

Indirect Calorimetry. During the final 30 min of the basal period and the clamp, indirect calorimetry was performed using the ventilated hood technique (Deltatrack Metabolic Monitor Sensor, Anaheim, CA) to assess rates of whole-body oxidative glucose and lipid metabolism (11, 43, 46).

Muscle Biopsy. A muscle biopsy from vastus lateralis was obtained 1 h before the start of the euglycemic-hyperinsulinemic clamp, as previously described (8). All muscle biopsy samples were stored in liquid nitrogen until assay.

Weight-Loss Protocol. Upon completion of the baseline study, the subjects began a weight-loss regimen with a caloric intake of 1,200 Kcal/d. This diet consisted mainly of liquid meals containing 43% protein, 49% percent carbohydrate, 7% fat, and 0.1% dietary fiber (Medibase, Monterey, CA) supplemented with a moderate amount of fruit and vegetables. Once a week during the weight-loss period vital signs were obtained, plasma glucose, insulin, and electrolytes were measured, and the subjects were weighed. All subjects were selected to be sedentary and during this study they were instructed not to change their daily activities or exercise. The average weight loss period was 9 ± 2 wk (range: 5–20 wk), which was followed by a 2-wk stabilization period before the post weight loss studies. The endpoint of the study was a weight loss of ~10% of the initial body weight.

Postweight-Loss Studies. Following weight loss the subjects were placed on a weight maintenance diet for approximately 2 wk until the baseline tests were completed. This regular diet consisted of 55% carbohydrate, 15% protein, 30% fat, 30 Kcal/kg body weight, with the calories evenly divided between breakfast, lunch, and dinner.

Metabolite and Adipocytokine Analyses. Plasma glucose and lactate concentrations were measured using a Yellow Springs STAT 2700 Analyzer (Yellow Springs Instruments). Plasma immunoreactive insulin, C-peptide, leptin, and adiponectin concentrations were measured with double-antibody radioimmuno assay techniques using a commercially available kit (Diagnostic Systems Laboratories). Plasma fatty acid and glycerol concentrations were measured enzymatically (24). Plasma concentrations of IL-6 and TNF-α were measured using Quantine High Sensitivity kits (R&D Systems) and total adiponectin concentrations were measured using a double-antibody RIA kit (Linco). Plasma concentrations of acylcarnitines were measured by LC-MS/MS, as previously described (47). Plasma amino acid concentrations were measured as the trifluoro-acetamide n-butyl ester derivatives (1), using GC-MS (HP 5973MSD; Hewlett-Packard). The amino acid profile was obtained

from 20 μL plasma by spiking the plasma with a known concentration of ^{13}C or deuterium-labeled amino acids chosen to avoid interference with any labeled amino acids. Concentrations of all amino acids were then determined by scanning the appropriate mass range 100–500 Da and calculating the isotope dilution of the enriched amino acid standards (48). The enrichments of plasma [6,6-$^2H_2$]glucose and [$^2H_5$]glycerol were measured using GC-MS, as previously described (11, 46).

Transmission Electron Microscopy. For electron microscopic examination, individual muscle samples were fixed in 2.5% (vol/vol) glutaraldehyde in 0.1 M cacodylate buffer (pH 7.4) at 4 °C overnight, postfixed, dehydrated, and embedded in epoxy resin, as previously described (8). Ultrathin sections (60 nm) were stained with 2% (vol/vol) uranyl acetate and lead citrate, and examined in a Tecnai 12 Biotwin electron microscope. For each individual muscle, four random sections were examined and, from each section, five random pictures were taken at a magnification of 6,800 and printed at a final magnification of 18,500. The volume densities of lipid droplets and mitochondria were estimated using the point counting method in a blinded fashion. For each set of five pictures, average volume density was calculated and the mean of both values used to estimate the volume density for each individual muscle (8).

Calculations. Statistical differences between before and after the weight loss were performed using the Student *t* test and ANOVA with Scheffés post hoc testing, when appropriate.

ACKNOWLEDGMENTS. We thank Donna Caseria, Carolyn Canonica, Christopher Cunningham, Mario Kahn, Yanna Kosover, Irina Smolgovsky, Mikhail Smolgovsky, Donna D'Eugenio, Gina Solomon, Caitlyn Schalich, Nadine Schatzkes, Morven Graham, and the staff of the Yale Center for Clinical Investigation Hospital Research Unit for their technical support, as well as all the volunteers for their participation in these studies. These studies were supported by US Public Health Service Grants AG-23686 (to K.F.P.), DK-49230 (to G.I.S.), RR-024139, DK-45735, and by a Distinguished Clinical Scientist Award from the American Diabetes Association (to K.F.P.).

1. Lillioja S, et al. (1988) Impaired glucose tolerance as a disorder of insulin action. Longitudinal and cross-sectional studies in Pima Indians. *N Engl J Med* 318:1217–1225.
2. Lillioja S, et al. (1993) Insulin resistance and insulin secretory dysfunction as precursors of non-insulin-dependent diabetes mellitus. Prospective studies of Pima Indians. *N Engl J Med* 329:1988–1992.
3. Warram JH, Martin BC, Krolewski AS, Soeldner JS, Kahn CR (1990) Slow glucose removal rate and hyperinsulinemia precede the development of type II diabetes in the offspring of diabetic parents. *Ann Intern Med* 113:909–915.
4. Zimmet P, Alberti KG, Shaw J (2001) Global and societal implications of the diabetes epidemic. *Nature* 414:782–787.
5. Rothman DL, Shulman RG, Shulman GI (1992) 31P nuclear magnetic resonance measurements of muscle glucose-6-phosphate. Evidence for reduced insulin-dependent muscle glucose transport or phosphorylation activity in non-insulin-dependent diabetes mellitus. *J Clin Invest* 89:1069–1075.
6. Perseghin G, et al. (1996) Increased glucose transport-phosphorylation and muscle glycogen synthesis after exercise training in insulin-resistant subjects. *N Engl J Med* 335:1357–1362.
7. Cline GW, et al. (1999) Impaired glucose transport as a cause of decreased insulin-stimulated muscle glycogen synthesis in type 2 diabetes. *N Engl J Med* 341:240–246.
8. Morino K, et al. (2005) Reduced mitochondrial density and increased IRS-1 serine phosphorylation in muscle of insulin-resistant offspring of type 2 diabetic parents. *J Clin Invest* 115:3587–3593.
9. Krssak M, et al. (1999) Intramyocellular lipid concentrations are correlated with insulin sensitivity in humans: A 1H NMR spectroscopy study. *Diabetologia* 42:113–116.
10. Jacob S, et al. (1999) Association of increased intramyocellular lipid content with insulin resistance in lean nondiabetic offspring of type 2 diabetic subjects. *Diabetes* 48: 1113–1119.
11. Petersen KF, Dufour S, Befroy D, Garcia R, Shulman GI (2004) Impaired mitochondrial activity in the insulin-resistant offspring of patients with type 2 diabetes. *N Engl J Med* 350:664–671.
12. Itani SI, Ruderman NB, Schmieder F, Boden G (2002) Lipid-induced insulin resistance in human muscle is associated with changes in diacylglycerol, protein kinase C, and IkappaB-alpha. *Diabetes* 51:2005–2011.
13. Perseghin G, et al. (1999) Intramyocellular triglyceride content is a determinant of in vivo insulin resistance in humans: A 1H-13C nuclear magnetic resonance spectroscopy assessment in offspring of type 2 diabetic parents. *Diabetes* 48:1600–1606.
14. Shulman GI (2000) Cellular mechanisms of insulin resistance. *J Clin Invest* 106:171–176.
15. Morino K, Petersen KF, Shulman GI (2006) Molecular mechanisms of insulin resistance in humans and their potential links with mitochondrial dysfunction. *Diabetes* 55(Suppl 2):S9–S15.
16. Samuel VT, Petersen KF, Shulman GI (2010) Lipid-induced insulin resistance: Unravelling the mechanism. *Lancet* 375:2267–2277.
17. Olefsky JM (2009) IKKepsilon: A bridge between obesity and inflammation. *Cell* 138: 834–836.
18. Olefsky JM, Glass CK (2010) Macrophages, inflammation, and insulin resistance. *Annu Rev Physiol* 72:219–246.
19. Hotamisligil GS (2006) Inflammation and metabolic disorders. *Nature* 444:860–867.
20. Lin HV, et al. (2007) Adiponectin resistance exacerbates insulin resistance in insulin receptor transgenic/knockout mice. *Diabetes* 56:1969–1976.
21. Newgard CB, et al. (2009) A branched-chain amino acid-related metabolic signature that differentiates obese and lean humans and contributes to insulin resistance. *Cell Metab* 9:311–326.
22. Wang TJ, et al. (2011) Metabolite profiles and the risk of developing diabetes. *Nat Med* 17:448–453.
23. Koves TR, et al. (2008) Mitochondrial overload and incomplete fatty acid oxidation contribute to skeletal muscle insulin resistance. *Cell Metab* 7:45–56.
24. Petersen KF, et al. (2006) Increased prevalence of insulin resistance and nonalcoholic fatty liver disease in Asian-Indian men. *Proc Natl Acad Sci USA* 103:18273–18277.
25. Bell JA, et al. (2010) Lipid partitioning, incomplete fatty acid oxidation, and insulin signal transduction in primary human muscle cells: Effects of severe obesity, fatty acid incubation, and fatty acid translocase/CD36 overexpression. *J Clin Endocrinol Metab* 95:3400–3410.
26. Shoelson SE, Herrero L, Naaz A (2007) Obesity, inflammation, and insulin resistance. *Gastroenterology* 132:2169–2180.
27. Petersen KF, et al. (2002) Leptin reverses insulin resistance and hepatic steatosis in patients with severe lipodystrophy. *J Clin Invest* 109:1345–1350.
28. Petersen KF, et al. (2005) Reversal of nonalcoholic hepatic steatosis, hepatic insulin resistance, and hyperglycemia by moderate weight reduction in patients with type 2 diabetes. *Diabetes* 54:603–608.
29. Lim EL, et al. (2011) Reversal of type 2 diabetes: normalisation of beta cell function in association with decreased pancreas and liver triacylglycerol. *Diabetologia* 54: 2506–2514.
30. Yu C, et al. (2002) Mechanism by which fatty acids inhibit insulin activation of insulin receptor substrate-1 (IRS-1)-associated phosphatidylinositol 3-kinase activity in muscle. *J Biol Chem* 277:50230–50236.
31. Summers SA (2006) Ceramides in insulin resistance and lipotoxicity. *Prog Lipid Res* 45: 42–72.
32. Choi CS, et al. (2008) Paradoxical effects of increased expression of PGC-1alpha on muscle mitochondrial function and insulin-stimulated muscle glucose metabolism. *Proc Natl Acad Sci USA* 105:19926–19931.
33. Samuel VT, et al. (2004) Mechanism of hepatic insulin resistance in non-alcoholic fatty liver disease. *J Biol Chem* 279:32345–32353.
34. Samuel VT, et al. (2007) Inhibition of protein kinase C epsilon prevents hepatic insulin resistance in nonalcoholic fatty liver disease. *J Clin Invest* 117:739–745.
35. Li Y, et al. (2004) Protein kinase C Theta inhibits insulin signaling by phosphorylating IRS1 at Ser(1101). *J Biol Chem* 279:45304–45307.
36. Høeg LD, et al. (2011) Lipid-induced insulin resistance affects women less than men and is not accompanied by inflammation or impaired proximal insulin signaling. *Diabetes* 60:64–73.
37. Befroy DE, et al. (2007) Impaired mitochondrial substrate oxidation in muscle of insulin-resistant offspring of type 2 diabetic patients. *Diabetes* 56:1376–1381.
38. Mootha VK, et al. (2003) PGC-1alpha-responsive genes involved in oxidative phosphorylation are coordinately downregulated in human diabetes. *Nat Genet* 34: 267–273.
39. Patti ME, et al. (2003) Coordinated reduction of genes of oxidative metabolism in humans with insulin resistance and diabetes: Potential role of PGC1 and NRF1. *Proc Natl Acad Sci USA* 100:8466–8471.
40. Morino K, et al. (2012) Regulation of mitochondrial biogenesis by lipoprotein lipase in muscle of insulin-resistant offspring of parents with type 2 diabetes. *Diabetes* 61: 877–887.
41. Wang YX, et al. (2004) Regulation of muscle fiber type and running endurance by PPARdelta. *PLoS Biol* 2:e294.
42. Matsuda M, DeFronzo RA (1999) Insulin sensitivity indices obtained from oral glucose tolerance testing: Comparison with the euglycemic insulin clamp. *Diabetes Care* 22: 1462–1470.
43. Petersen KF, et al. (1998) 13C/31P NMR studies on the mechanism of insulin resistance in obesity. *Diabetes* 47:381–386.
44. Gruetter R (1993) Automatic, localized in vivo adjustment of all first- and second-order shim coils. *Magn Reson Med* 29:804–811.
45. Rabøl R, Petersen KF, Dufour S, Flannery C, Shulman GI (2011) Reversal of muscle insulin resistance with exercise reduces postprandial hepatic de novo lipogenesis in insulin resistant individuals. *Proc Natl Acad Sci USA* 108:13705–13709.
46. Petersen KF, et al. (2003) Mitochondrial dysfunction in the elderly: Possible role in insulin resistance. *Science* 300:1140–1142.
47. Vernez L, Wenk M, Krähenbühl S (2004) Determination of carnitine and acylcarnitines in plasma by high-performance liquid chromatography/electrospray ionization ion trap tandem mass spectrometry. *Rapid Commun Mass Spectrom* 18:1233–1238.
48. Leimer KR, Rice RH, Gehrke CW (1977) Complete mass spectra of *N*-trifluoroacetyl-n-butyl esters of amino acids. *J Chromatogr A* 141:121–144.